JACS
JOURNAL OF THE AMERICAN CHEMICAL SOCIETY

ARTICLE

pubs.acs.org/JACS

Chemical Wiring and Soldering toward All-Molecule Electronic Circuitry

Yuji Okawa,*[,†] Swapan K. Mandal,[†] Chunping Hu,[†] Yoshitaka Tateyama,[†,‡] Stefan Goedecker,[§] Shigeru Tsukamoto,[†,||] Tsuyoshi Hasegawa,[†] James K. Gimzewski,[†,⊥] and Masakazu Aono[†]

[†]International Center for Materials Nanoarchitectonics, National Institute for Materials Science, Tsukuba, Ibaraki 305-0044, Japan

[‡]PRESTO and CREST, JST, Kawaguchi, Saitama 332-0012, Japan

[§]Department of Physics and Astronomy, University of Basel, 4056 Basel, Switzerland

[||]Peter Grünberg Institut, Forschungszentrum Jülich and JARA, D-52425 Jülich, Germany

[⊥]California NanoSystems Institute at UCLA, Los Angeles, California 90095, United States

Supporting Information

ABSTRACT: Key to single-molecule electronics is connecting functional molecules to each other using conductive nanowires. This involves two issues: how to create conductive nanowires at designated positions, and how to ensure chemical bonding between the nanowires and functional molecules. Here, we present a novel method that solves both issues. Relevant functional molecules are placed on a self-assembled monolayer of diacetylene compound. A probe tip of a scanning tunneling microscope is then positioned on the molecular row of the diacetylene compound to which the functional molecule is adsorbed, and a conductive polydiacetylene nanowire is fabricated by initiating chain polymerization by stimulation with the tip. Since the front edge of chain polymerization necessarily has a reactive chemical species, the created polymer nanowire forms chemical bonding with an encountered molecular element. We name this spontaneous reaction "chemical soldering". First-principles theoretical calculations are used to investigate the structures and electronic properties of the connection. We demonstrate that two conductive polymer nanowires are connected to a single phthalocyanine molecule. A resonant tunneling diode formed by this method is discussed.

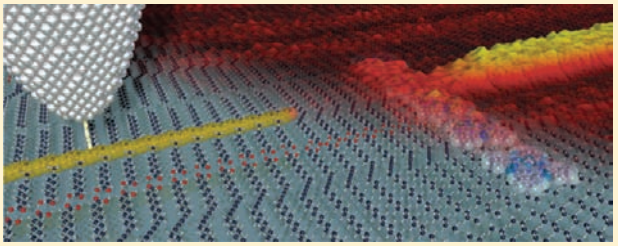

INTRODUCTION

In single-molecule electronics, each organic molecule performs the basic functions of electronics such as rectification, amplification, and storage. Single-molecule electronics will enable us to develop cheaper, higher-performance, and more-ecological alternatives to conventional silicon-based devices. Hence, many efforts have been made to realize single-molecule electronics,[1−16] and it is still a very active area of research.[3−5] The concept is now realized for individual components,[4−12] but it is still impossible to fabricate a practical single-molecule integrated circuit. One of the problems is the lack of viable methods for wiring each functional molecule. Despite many reported efforts on connecting metal electrodes directly to single molecules,[4−8] it remains very difficult to reduce the width of metal wires to that of single molecules, so it is difficult to reduce the total size of molecular circuits. One solution is to connect each molecule with a single conductive polymer instead of a metal wire, but there are currently no reports of a practical method for achieving this.

We should also note that the lack of a viable method for wiring is not the only problem for realizing single-molecule integrated circuit. On a more fundamental level, it has been shown that, with single-molecule circuits, it is not possible to decompose a larger molecule into different parts, where some parts act as wires and others as active devices. This is due to the wave propagation nature of electron transport in the tunneling regime. Therefore, circuit design strategies from classical electronics cannot be simply scaled down when the circuit is supposed to be larger than the usual demonstration piece of one diode or transistor embedded in a wire. Hence, new architectural schemes are needed for circuit design.[3,13−16] The fabrication and evaluation of a large molecule, in which a functional molecule and conjugated polymers are connected, will be a great help to establish strategies for proper circuit design.

In order to develop a viable method to connect conductive polymer nanowires to each functional molecule, we have to solve two issues: how to create polymer nanowires at designated positions, and how to ensure chemical bonding between the nanowires and functional molecules. The first issue has been solved using nanoscale controlled chain polymerization,[17−20] which is discussed later. The second issue, connection via a firm covalent bond between the functional molecule and the conductive

Received: December 28, 2010
Published: May 06, 2011

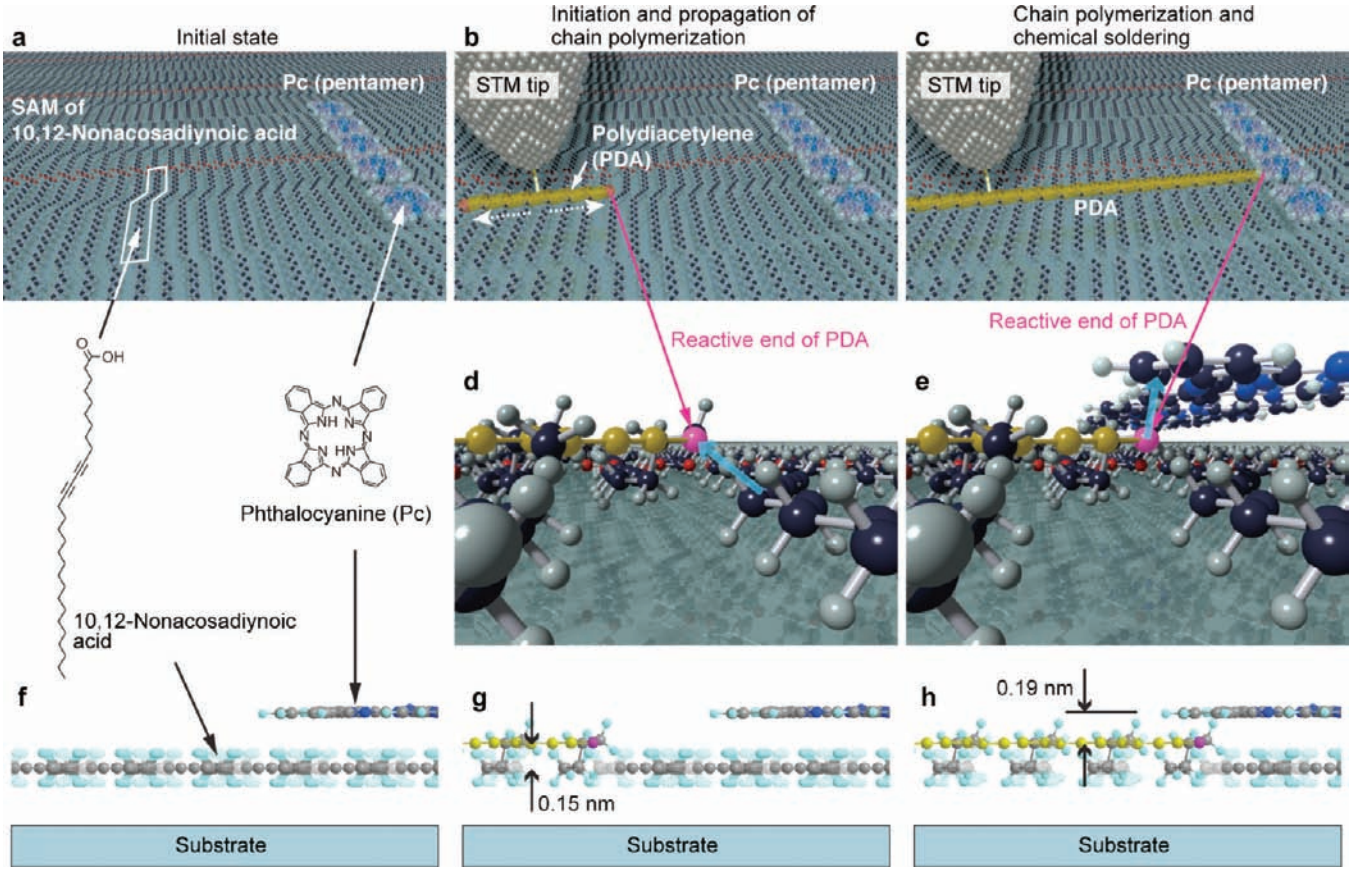

Figure 1. Schematic images showing chemical soldering. (a) Illustration of phthalocyanine molecules adsorbed to a self-assembled monolayer (SAM) of 10,12-nonacosadiynoic acid molecules. (b) Chain polymerization is initiated using an STM tip. (c) The polymer chain reaches the adsorbed molecule, and spontaneous chemical bond formation occurs. (d) The adjacent monomer molecule reacts with the reactive end of the PDA (magenta sphere), as indicated by the light blue arrow. (e) Lifted-up structure of the PDA enables the reactive end to approach the adsorbed molecule. (f–h) Side views of the models. The PDA backbone (yellow spheres) protrudes by 0.15 nm.

polymer, is also requisite for reliable electronic properties because of the thermal fluctuation tolerance of the positions of molecules. Chemistry will play a key role in achieving this because it is necessary to control single-molecule covalent chemistry[21−32] on solid substrates.

In a simple idea for connecting conductive polymers to a functional molecule, it is expected that the connection will be achieved by first synthesizing the polymers and the functional molecule separately, and then positioning them on a substrate and chemically bonding them together. Barner et al. deposited single chains of a dendronized polymer with peripheral azide groups on a solid substrate. Using a scanning force microscope tip, they moved one polymer chain next to another polymer chain, and then used ultraviolet light to photochemically connect them.[25] The dendronized polymer, however, was not conductive. Several covalently bonded polymers synthesized on a substrate have also been reported.[26−32] However, there have been no demonstrations showing a connection to another functional molecule due to the difficulty in positioning the polymers accurately. Here, we propose a new approach shown schematically in Figure 1 and Movie S1 in Supporting Information. Monomer molecules of the diacetylene compound (R−C≡C−C≡C−R′, where C≡C−C≡C is the diacetylene moiety and R and R′ are substituent groups) are deposited on a cleaved face of highly oriented pyrolytic graphite (HOPG) and form a self-assembled monolayer (SAM). In the case of 10,12-nonacosadiynoic acid, which was used in the present work, R is $CH_3(CH_2)_{15}-$ and R′ is $-(CH_2)_8COOH$. A small quantity of functional molecules is then deposited on the SAM (Figure 1a,f). [In Figure 1, a nanocluster composed of five metal-free-phthalocyanine molecules (H_2Pc pentamer) is drawn as the functional molecule, which is discussed later in detail.] After that, the tip of a scanning tunneling microscope (STM) is positioned on the molecular row of the diacetylene compound to which the functional molecule is adsorbed, and the diacetylene moiety beneath the tip is stimulated by a pulsed bias voltage. This stimulation initiates the chain polymerization of the diacetylene moiety; thus, a single polydiacetylene (PDA) chain ($(=RC-C\equiv C-CR'=)_n$) is fabricated along the row (Figure 1b), which is described in previous reports.[17−20] The PDA chain obtained is a conjugated linear polymer of sub-micrometer length. Following charge carrier injection by chemical doping[33] or by an applied electric field,[34,35] the PDA chain should function as an electrically conductive nanowire.

The PDA chain obtained has a "lifted-up" structure,[36] in which the PDA backbone is raised by 0.15 nm as shown in Figure 1g. During the chain polymerization, there are reactive chemical species (carbenes or radicals) at the propagating ends of the chain.[37,38] Although the lifted-up structure places the reactive end of the chain 0.15 nm above the monomer adjacent to the polymer (Figure 1d,g), the chain polymerization propagates because the

vibrational excitation of the PDA and monomer molecules enables the end of the chain to react with the adjacent monomer molecule. When the polymer chain reaches the adsorbed functional molecule (Figure 1c), the lifted-up structure of PDA enables the reactive end to approach the adsorbed molecule. This is shown in Figure 1e,h. Assuming the distance between the phthalocyanine and the alkyl side chains of the diacetylene compound is the same as that between the graphite and the alkyl chains, 0.34 nm,[39] the height difference between the phthalocyanine and the PDA backbone is deduced as 0.19 nm. This is only 0.04 nm greater than the height difference between the reactive end of the propagating PDA chain and the adjacent monomer molecule. Therefore, the reactive end of the chain will also react with the adsorbed functional molecule to form a covalent bond spontaneously. We name this spontaneous reaction "chemical soldering".

The functional molecules we used were metal-free-phthalocyanine (H_2Pc), copper phthalocyanine (CuPc), and zinc phthalocyanine (ZnPc). Phthalocyanines are planar functional dyes and have drawn considerable attention, due to their outstanding electronic and optical properties,[40] allowing their use as switches[10] and light-emitting devices.[41−43] Furthermore, the stabilization of nanometer-sized domains of CuPc on top of alkane molecular layers adsorbed on graphite substrates[44,45] enables us to observe each molecule using STM at room temperature.

EXPERIMENTAL SECTION

To make a sample, a thin film of 10,12-nonacosadiynoic acid molecules on the surface of purified water was transferred to a freshly cleaved surface of HOPG (SPI-2 or ZYH grade) by nearly horizontal dipping. The sample was then dried by storing it in a desiccator for 4−18 h at room temperature in the dark. The sample was then placed in a vacuum chamber, and phthalocyanine was deposited under a 7×10^{-4} Pa vacuum at about 295 K. The deposition rate was monitored using a quartz crystal deposition monitor. The STM experiments were performed in air at room temperature using a NanoScope STM system with Pt−Ir tips operated in constant current mode. The sample bias voltage and the tunneling current for observation were typically −1 V and 30−50 pA, respectively.

RESULTS AND DISCUSSION

Figure 2a shows an STM image of a pristine SAM of 10,12-nonacosadiynoic acid on a graphite substrate. After about 0.1 monolayer coverage of CuPc was deposited on it, small protrusions appeared, which are shown in Figure 2b. The smallest protrusions (labeled "Monomer" in Figure 2b) are 1.3−2.0 nm in diameter, which corresponds to the size of a CuPc molecule. Therefore, these smallest protrusions are single CuPc molecules (monomers) adsorbed to and stabilized on the alkyl side chains of the 10,12-nonacosadiynoic acid. Figure 2b also shows that the nanoclusters of CuPc molecules adsorbed to the SAM. The nanocluster labeled "Dimer" consists of two CuPc molecules. The nanocluster labeled "Pentamer" consists of five CuPc molecules, which is shown in Figure 2d, and is adsorbed across two rows of 10,12-nonacosadiynoic acid molecules. Pentamers of phthalocyanine are frequently observed (Figure 2c), which indicates that the pentamer is a relatively stable structure on the SAM of the 10,12-nonacosadiynoic acid. Two of the CuPc molecules in a pentamer are adsorbed just above the diacetylene moieties of 10,12-nonacosadiynoic acid, which is shown

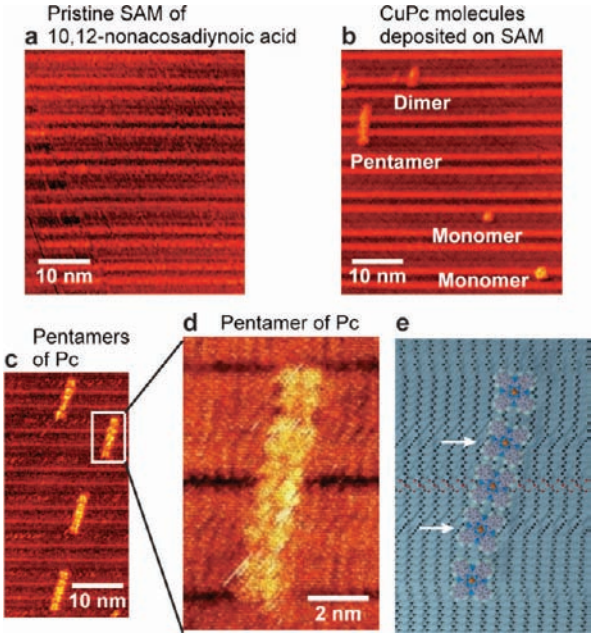

Figure 2. STM images of phthalocyanine nanoclusters. (a) STM image of a pristine SAM of 10,12-nonacosadiynoic acid molecules. (b) STM image obtained after depositing a small quantity of CuPc molecules on the SAM shown in (a). Monomers, a dimer, and a pentamer of CuPc are evident. (c) STM image of pentamers of CuPc. (d) Magnified STM image of a CuPc pentamer. (e) Schematic model of a pentamer of phthalocyanine. The two phthalocyanine molecules indicated by arrows are adsorbed just above the diacetylene moiety.

schematically in Figure 2e. This configuration enables these phthalocyanine molecules to sufficiently approach the reactive end of the PDA. Monomers, dimers, and pentamers of H_2Pc and ZnPc molecules were also seen on the 10,12-nonacosadiynoic acid SAMs.

The chemical soldering process is shown in Figure 3. An STM tip was positioned above the row of 10,12-nonacosadiynoic acid to which an H_2Pc pentamer was adsorbed, and chain polymerization was initiated by applying a pulsed sample bias voltage (−3.8 V for 5 μs). Figure 3a shows an STM image obtained after applying the pulsed voltage in which the resultant PDA chain (bright line in the STM image) is connected to the H_2Pc molecule. We also succeeded in connecting single PDA chains to CuPc and ZnPc pentamers. We repeated this process and connected single PDA chains to phthalocyanine pentamers more than 60 times. Examining the STM images taken near the connecting point in detail, we found that the PDA backbone showed two types of image contrast in that area. In one (type A, shown in Figure 3a), the image contrast of the PDA backbone near the connecting point decreases. In the other (type B, shown in Figure 3c), the image contrast of the PDA backbone is almost constant. The height cross sections along the lines in Figure 3a,c are shown in Figure 3b, which illustrates the difference between the two types. About 70% of the STM images we obtained showed type A contrast. We also noted that, although in the lifted-up structure the PDA backbone was raised only 0.15 nm, STM images show that the PDA backbone is more than 0.3 nm above the diacetylene monomers[46] (see Figure 3b). This indicates that the height of the PDA backbone observed in STM images was greatly influenced by the conjugated electronic state of the backbone.

dx.doi.org/10.1021/ja111673x |J. Am. Chem. Soc. 2011, 133, 8227–8233

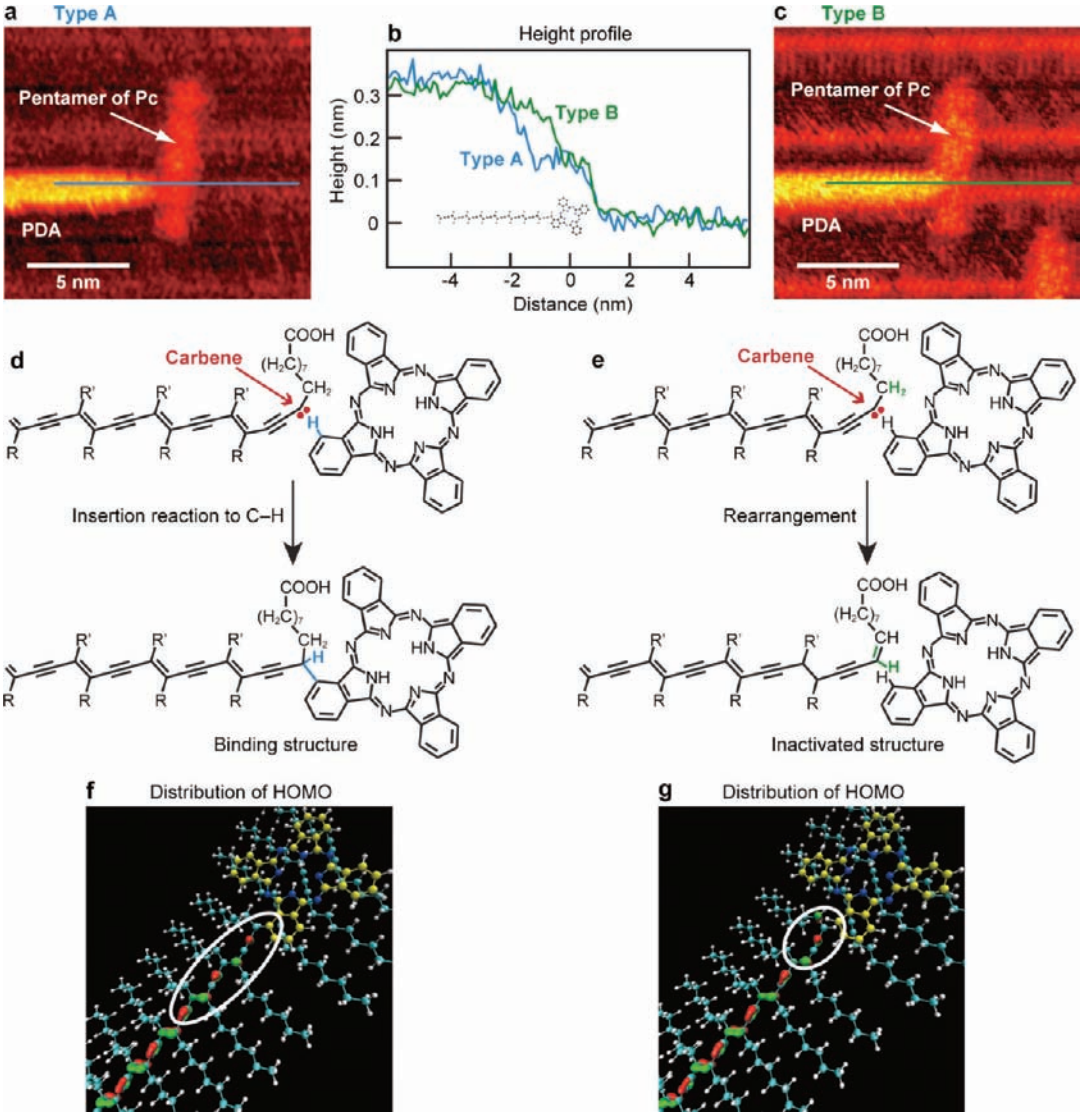

Figure 3. Demonstration of chemical soldering and possible chemical reactions. STM images (a) and (c) are obtained after applying pulsed bias voltages on the row of 10,12-nonacosadiynoic acid to which an H_2Pc pentamer is adsorbed. Fabricated PDA chains are imaged as bright lines. (a) STM image showing type A image contrast. The image contrast of the PDA backbone near the connecting point decreases. (b) Height cross sections along the lines in (a) and (c). (c) STM image showing type B image contrast. The image contrast of the PDA backbone is almost constant. (d) Chemical reaction resulting in the binding structure. The reactive end of PDA is inserted into a C−H bond of phthalocyanine. (e) Chemical reaction resulting in the inactivated structure. Through this rearrangement, a hydrogen atom is transferred from the alkyl side chain to the terminal carbon atom of PDA. (f,g) Optimized structure models and calculated HOMO densities for the binding and the inactivated structures, respectively. Light blue, yellow, blue, and white spheres show carbon atoms in the monomer/polymer molecules, carbon atoms in the phthalocyanine molecule, nitrogen atoms, and hydrogen atoms, respectively. Red and green isosurfaces show the calculated distribution of HOMO density. White ovals indicate the regions of smaller HOMO density.

To clarify the origin of these two types of image contrast, we investigated the stability of possible configurations of the polymer and phthalocyanine. For that purpose, we carried out structural optimizations of several possible configurations of polymers with/without binding to phthalocyanine via the density-functional first-principles method with a wavelet basis set (BigDFT) designed for large-scale calculations[47] (see Supporting Information for details of the calculations). We found that the binding structure gives the lowest energy among calculated structures, which is shown in Figure 3d,f. In this structure, the active-carbon end of the polymer pulls the nearest hydrogen atom from phthalocyanine and binds to a carbon atom in phthalocyanine, which is shown in Figure 3d. This reaction corresponds to the insertion reaction of carbene into a C−H bond.[48] The calculated distribution of highest-occupied-molecular-orbital (HOMO) density is shown as red and green isosurfaces in Figure 3f. We found that the density in the two or three units of the polymer (indicated by a white oval in Figure 3f) closest to the connecting point is smaller than that of units in the central part of the polymer. Since the STM images mainly reflect the density of the HOMO, we conclude that this binding structure between the polymer and the phthalocyanine produces the type A contrast shown in Figure 3a.

dx.doi.org/10.1021/ja111673x |*J. Am. Chem. Soc.* 2011, 133, 8227–8233

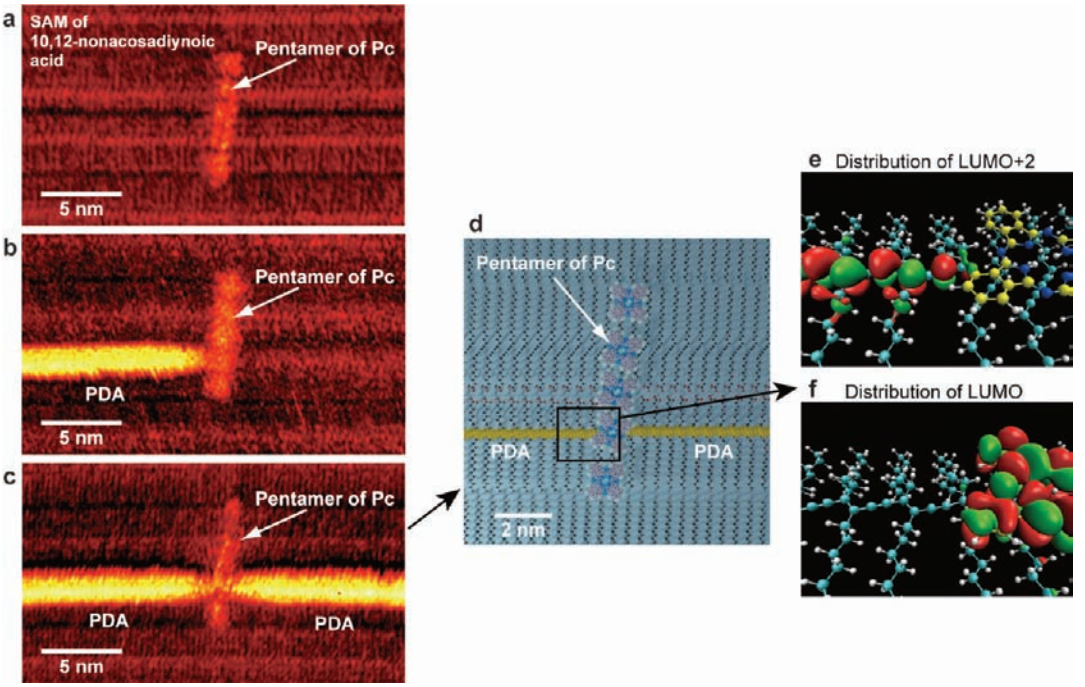

Figure 4. Connecting two PDA chains to a single phthalocyanine molecule. (a) STM image of an H_2Pc pentamer on a SAM of 10,12-nonacosadiynoic acid. (b) STM image obtained after initiating chain polymerization. Fabricated PDA chain, which is seen as a bright line, is connected to an H_2Pc molecule. (c) STM image showing two PDA chains connected to a single H_2Pc molecule. (d) Schematic model of (c). (e,f) Red and green isosurfaces show the calculated distributions of LUMO+2 and LUMO densities.

We also investigated a structure where a hydrogen atom from the alkyl side chain of the polymer transfers to terminate the neighbor active-carbon end (1,2-rearrangement),[48] as shown in Figure 3e. We hereafter refer this structure as "inactivated". In this case, there is no bond between the polymer and the phthalocyanine, because the bonding with the transferred hydrogen atom inactivates the carbon end of the polymer chain. We found that this structure is metastable, and that its calculated total energy is 0.8 eV greater than that of the binding structure. The HOMO density calculated for this structure is shown in Figure 3g, where only the end unit of the polymer has a HOMO density smaller than that of units in the central part of the polymer. We thus attribute the type B image contrast (Figure 3c) to this inactivated structure. These assignments are consistent with the observed structural stability in that the type A contrast is more common than the type B contrast. Thus, the polymer connection to phthalocyanine (chemical soldering) is the main reaction, so the subsequent discussions in this article will focus on the binding structure.

A demonstration of connecting two polymer chains to a single phthalocyanine molecule is presented in Figure 4 and Movie S1 in Supporting Information. Figure 4a shows an STM image of an H_2Pc pentamer adsorbed to a 10,12-nonacosadiynoic acid SAM. Chain polymerization was initiated by applying a pulsed bias voltage (−3.8 V for 5 μs) to the row of 10,12-nonacosadiynoic acid to which the H_2Pc pentamer is adsorbed, and the resultant PDA chain (bright line in Figure 4b) was connected to the H_2Pc molecule. The second PDA chain was then connected to the same single H_2Pc molecule, which is shown in Figure 4c, by applying a pulsed bias voltage to the same row of diacetylene molecules but on the other side of the adsorbed H_2Pc molecule. Figure 4d shows a schematic model of this. STM image contrast around the connecting points shown in Figure 4c indicates that both polymer chains are connected to the H_2Pc molecule via binding structures.

Figure 4e,f shows the calculated distribution of the third lowest-unoccupied-molecular-orbital (LUMO+2) and the lowest-unoccupied-molecular-orbital (LUMO) densities, which are localized on PDA and H_2Pc, respectively (see also Figure 5a). These figures show that the conjugated electronic states do not spread over the PDA−H_2Pc−PDA system, because the terminal carbon atom of the polymer is converted to sp^3 by the insertion reaction. Though the sp^3 carbon atom at the junction acts as a potential energy barrier to electron flow, we can utilize the barrier as a component of molecular devices, which is discussed later.

Figure 5a shows a schematic energy level diagram of the PDA−ZnPc−PDA system generated from the density-functional first-principles calculation for the binding structure of PDA−ZnPc system. The calculation used the PDA consisting of eight polymer units (see Supporting Information). Although calculation for the finite size gives the discrete energy levels, which are indicated by the lines in Figure 5a, continuous valence band (VB) and conduction band (CB) for PDA chains of infinite length are assumed as indicated by the pink-colored boxes in the figure. When negative or positive charges are injected to the polydiacetylene chain, structural deformation takes place in the polymer backbone during energy relaxation. These structural deformations combined with charges are called polarons or bipolarons, which are the charge carriers in the polydiacetylene chain.[34,49] The polaronic states are present within the parent band gap of polydiacetylene, as indicated in Figure 5a. From scanning tunneling spectroscopy (STS) measurements,[34] the position of negative polaronic state (P^-) is estimated to be about 0.3 eV lower than the bottom of CB. Though polarons (or bipolarons) cannot pass through the sp^3 carbon atom at the PDA−phthalocyanine junction, they can approach the adjoining

dx.doi.org/10.1021/ja111673x | J. Am. Chem. Soc. 2011, 133, 8227–8233

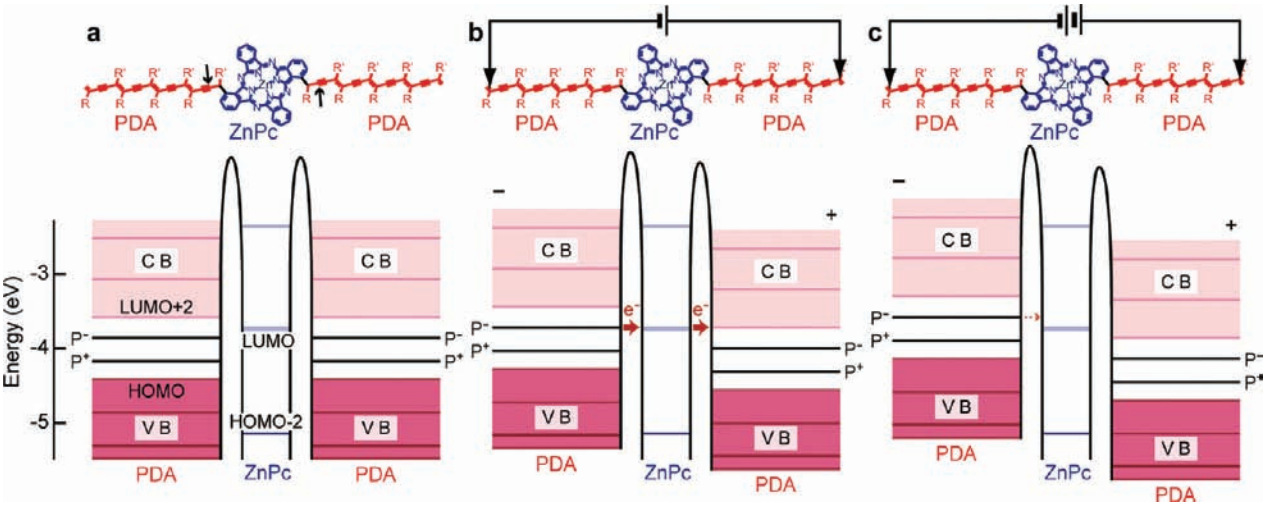

Figure 5. Energy level diagram and possible application to molecular resonant-tunneling diode. (a) Energy level diagram of PDA–ZnPc–PDA system. Lines show calculated energy levels. Continuous valence band (VB) and conduction band (CB) are assumed for PDA chains of infinite length. P^+ and P^- are positive and negative polaron states, respectively. A polaron can approach the carbon atom as indicated by the arrows in the molecular model. (b) Bias voltage is applied between two PDA chains. If the bias voltage is adjusted so that the energy of incoming electrons is equivalent to the energy level of ZnPc, electrons can flow from left to right through ZnPc, as indicated by the red arrows. (c) When the bias voltage is higher than the resonant voltage, the flow of electrons is restrained.

carbon atom, as indicated by arrows in the molecular model of Figure 5a, which are very close to the ZnPc molecule. Hence, charges can transfer from the polaronic state of PDA to the energy levels of phthalocyanine. Note that, if a polymer chain and a phthalocyanine molecule are separately deposited on a substrate, it will be very difficult to arrange them in such a close arrangement. In contrast, the tight positioning of PDA is spontaneously and accurately achieved in our chemical soldering method.

The PDA–ZnPc–PDA system (Figure 5a) may act as molecular-resonant-tunneling diode (RTD), which was previously demonstrated for the phenylene ethynylene–CH_2–benzene–CH_2–phenylene ethynylene molecule.[8,50] Namely, in Figure 5b, it can be seen that if the bias voltage is adjusted such that the energy of the incoming electrons is equivalent to the energy level of ZnPc ("in resonance"), an electron can directly tunnel from the left-hand region onto the ZnPc molecule. In this case, electrons can flow from left to right through the ZnPc. Thus, the RTD is switched on. If the bias voltage is lower or higher than this resonant voltage, the flow of electrons will be restrained (Figure 5c). In this case, the RTD is switched off. Such a molecular RTD could be a useful component of future single-molecule electronics. It should also be pointed out that the energy levels of phthalocyanine can be adjusted by selecting central metal atoms[43,51] or substituents,[52] such that we can design and control the electronic properties of the system.

Although we used graphite as the substrate in the demonstration presented here, the use of other substrates should be possible. For instance, similar linear PDA chains have been formed on a semiconducting MoS_2 substrate, using photopolymerization[46] or using STM-tip-induced-polymerization.[53] The formation of PDA chains on a molecular multilayer film,[19] which is an insulating layer, could also be useful.

CONCLUSION

In conclusion, we demonstrated a viable method for connecting single conductive polymer nanowires to a single functional molecule via covalent bonds, through spontaneous chemical reactions of the reactive carbon ends of the propagating polymer chains. We name this method "chemical soldering". In this demonstration we were able to connect two linear PDA chains to a single phthalocyanine molecule. This process and the resultant structures are suitable for the basic study of the chemistry and physics of nanometer-scale molecular systems. We believe that the structure could act as a molecular RTD device. We also believe that this method is applicable to many functional molecules in addition to phthalocyanine. Therefore, this method is useful for wiring each component of single-molecule devices (such as molecular diodes, switches, memory bits, and transistors) and thus represents a key step in advancing the development of future single-molecule circuits.

ASSOCIATED CONTENT

Supporting Information. Schematic movie showing the procedure for chemical soldering, and discussions on density-functional first-principles calculations. This material is available free of charge via the Internet at http://pubs.acs.org.

AUTHOR INFORMATION

Corresponding Author
okawa.yuji@nims.go.jp

ACKNOWLEDGMENT

The authors thank Y. Kuwahara, T. Uemura, J. P. Hill, and K. Ariga for helpful discussions and D. Takajo for support through sample preparation. This work was partially supported by JSPS KAKENHI (21310078).

REFERENCES

(1) Aviram, A.; Ratner, M. A. *Chem. Phys. Lett.* **1974**, *29*, 277–283.
(2) Andrews, D. Q.; Solomon, G. C.; Van Duyne, R. P.; Ratner, M. A. *J. Am. Chem. Soc.* **2008**, *130*, 17309–17319.

(3) Markussen, T.; Stadler, R.; Thygesen, K. S. *Nano Lett.* **2010**, *10*, 4260–4265.
(4) Díez-Pérez, I.; Hihath, J.; Lee., Y.; Yu, L.; Adamska, L.; Kozhushner, M. A.; Oleynik, I. I.; Tao, N. *Nat. Chem.* **2009**, *1*, 635–641.
(5) Song, H.; Kim, Y.; Jang, Y. H.; Jeong, H.; Reed, M. A.; Lee, T. *Nature* **2009**, *462*, 1039–1043.
(6) Park, J.; Pasupathy, A. N.; Goldsmith, J. I.; Chang, C.; Yaish, Y.; Petta, J. R.; Rinkoski, M.; Sethna, J. P.; Abruña, H. D.; McEuen, P. L.; Ralph, D. C. *Nature* **2002**, *417*, 722–725.
(7) Liang, W.; Shores, M. P.; Bockrath, M.; Long, J. R.; Park, H. *Nature* **2002**, *417*, 725–729.
(8) Reed, M. A. *Proc. IEEE* **1999**, *87*, 652–658.
(9) Joachim, C.; Gimzewski, J. K.; Aviram, A. *Nature* **2000**, *408*, 541–548.
(10) Liljeroth, P.; Repp, J.; Meyer, G. *Science* **2007**, *317*, 1203–1206.
(11) Donhauser, Z. J.; Mantooth, B. A.; Kelly, K. F.; Bumm, L. A.; Monnell, J. D.; Stapleton, J. J.; Price, D. W., Jr.; Rawlett, A. M.; Allara, D. L.; Tour, J. M.; Weiss, P. S. *Science* **2001**, *292*, 2303–2307.
(12) Piva, P. G.; DiLabio, G. A.; Pitters, J. L.; Zikovsky, J.; Rezeq, M.; Dogel, S.; Hofer, W. A.; Wolkow, R. A. *Nature* **2005**, *435*, 658–661.
(13) Stadler, R.; Ami, S.; Forshaw, M.; Joachim, C. *Nanotechnology* **2002**, *13*, 424–428.
(14) Stadler, R.; Forshaw, M.; Joachim, C. *Nanotechnology* **2003**, *14*, 138–142.
(15) Stadler, R.; Ami, S.; Forshaw, M.; Joachim, C. *Nanotechnology* **2003**, *14*, 722–732.
(16) Stadler, R.; Ami, S.; Joachim, C.; Forshaw, M. *Nanotechnology* **2004**, *15*, S115–S121.
(17) Okawa, Y.; Aono, M. *Nature* **2001**, *409*, 683–684.
(18) Okawa, Y.; Aono, M. *J. Chem. Phys.* **2001**, *115*, 2317–2322.
(19) Takajo, D.; Okawa, Y.; Hasegawa, T.; Aono, M. *Langmuir* **2007**, *23*, 5247–5250.
(20) Miura, A.; De Feyter, S.; Abdel-Mottaleb, M. M. S.; Gesquière, A.; Grim, P. C. M.; Moessner, G.; Sieffert, M.; Klapper, M.; Müllen, K.; De Schryver, F. C. *Langmuir* **2003**, *19*, 6474–6482.
(21) Lee, H. J.; Ho, W. *Science* **1999**, *286*, 1719–1722.
(22) Hla, S.-W.; Bartels, L.; Meyer, G.; Rieder, K.-H. *Phys. Rev. Lett.* **2000**, *85*, 2777–2780.
(23) Lopinski, G. P.; Wayner, D. D. M.; Wolkow, R. A. *Nature* **2000**, *406*, 48–51.
(24) Maksymovych, P.; Sorescu, D. C.; Jordan, K. D.; Yates, J. T., Jr. *Science* **2008**, *322*, 1664–1667.
(25) Barner, J.; Al-Hellani, R.; Schlüter, A. D.; Rabe, J. P. *Macromol. Rapid Commun.* **2010**, *31*, 362–367.
(26) Sakaguchi, H.; Matsumura, H.; Gong, H. *Nat. Mater.* **2004**, *3*, 551–557.
(27) Yang, L. Y. O.; Chang, C.-Z.; Liu, S.-H.; Wu, C.-G.; Yau, S. L. *J. Am. Chem. Soc.* **2007**, *129*, 8076–8077.
(28) Grill, L.; Dyer, M.; Lafferentz, L.; Persson, M.; Peters, M. V.; Hecht, S. *Nat. Nanotech.* **2007**, *2*, 687–691.
(29) Matena, M.; Riehm, T.; Stöhr, M.; Jung, T. A.; Gade, L. H. *Angew. Chem., Int. Ed.* **2008**, *47*, 2414–2417.
(30) Weigelt, S.; Busse, C.; Bombis, C.; Knudsen, M. M.; Gothelf, K. V.; Lægsgaard, E.; Besenbacher, F.; Linderoth, T. R. *Angew. Chem., Int. Ed.* **2008**, *47*, 4406–4410.
(31) Treier, M.; Richardson, N. V.; Fasel, R. *J. Am. Chem. Soc.* **2008**, *130*, 14054–14055.
(32) Lipton-Duffin, J. A.; Ivasenko, O.; Perepichka, D. F.; Rosei, F. *Small* **2009**, *5*, 592–597.
(33) Takami, K.; Kuwahara, Y.; Ishii, T.; Akai-Kasaya, M.; Saito, A.; Aono, M. *Surf. Sci.* **2005**, *591*, L273–L279.
(34) Akai-Kasaya, M.; Yamamoto, Y.; Saito, A.; Aono, M.; Kuwahara, Y. *Jpn. J. Appl. Phys.* **2006**, *45*, 2049–2052.
(35) Scott, J. C.; Samuel, J. D. J.; Hou, J. H.; Rettner, C. T.; Miller, R. D. *Nano Lett.* **2006**, *6*, 2916–2919.
(36) Okawa, Y.; Takajo, D.; Tsukamoto, S.; Hasegawa, T.; Aono, M. *Soft Matter* **2008**, *4*, 1041–1047.
(37) Neumann, W.; Sixl, H. *Chem. Phys.* **1981**, *58*, 303–312.
(38) Kollmar, C. *J. Chem. Phys.* **1993**, *98*, 7210–7228.
(39) Yang, T.; Berber, S.; Liu, J.-F.; Miller, G. P.; Tománek, D. *J. Chem. Phys.* **2008**, *128*, 124709.
(40) de la Torre, G.; Claessens, C. G.; Torres, T. *Chem. Commun.* **2007**, 2000–2015.
(41) Vincett, P. S.; Voigt, E. M.; Rieckhoff, K. E. *J. Chem. Phys.* **1971**, *55*, 4131–4140.
(42) Fujii, A.; Yoshida, M.; Ohmori, Y.; Yoshino, K. *Jpn. J. Appl. Phys.* **1996**, *35*, L37–L39.
(43) Hohnholz, D.; Steinbrecher, S.; Hanack, M. *J. Mol. Struct.* **2000**, *521*, 231–237.
(44) Xu, B.; Yin, S.; Wang, C.; Qiu, X.; Zeng, Q.; Bai, C. *J. Phys. Chem. B* **2000**, *104*, 10502–10505.
(45) Takajo, D.; Nemoto, T.; Ozaki, H.; Mazaki, Y.; Isoda, S. *Appl. Surf. Sci.* **2004**, *238*, 282–287.
(46) Giridharagopal, R.; Kelly, K. F. *ACS Nano* **2008**, *2*, 1571–1580.
(47) Genovese, L.; Neelov, A.; Goedecker, S.; Deutsch, T.; Ghasemi, S. A.; Willand, A.; Caliste, D.; Zilberberg, O.; Rayson, M.; Bergman, A.; Schneider, R. *J. Chem. Phys.* **2008**, *129*, 014109.
(48) Tomioka, H. *Advances in Carbene Chemistry*; The University of Nagoya Press: Nagoya, 2009.
(49) Heeger, A. J.; Kivelson, S.; Schrieffer, J. R.; Su, W.-P. *Rev. Mod. Phys.* **1988**, *60*, 781–850.
(50) Karzazi, Y.; Cornil, J.; Brédas, J. L. *J. Am. Chem. Soc.* **2001**, *123*, 10076–10084.
(51) Liao, M.-S.; Scheiner, S. *J. Chem. Phys.* **2001**, *114*, 9780–9791.
(52) Shinohara, H.; Tsaryova, O.; Schnurpfeil, G.; Wöhrle, D. *J. Photochem. Photobiol. A: Chem.* **2006**, *184*, 50–57.
(53) Mandal, S. K.; Okawa, Y.; Hasegawa, T.; Aono, M. *ACS Nano* **2011**, *5*, 2779–2786.